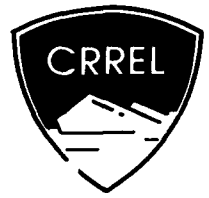AD-A247 868

CRREL

On the Use of an Artificial Snow Platform for WAM Tests

Donald G. Albert

January 1992

DTIC
S ELECTE D
MAR 18 1992
D

92-06850
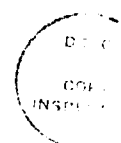
92 3 16 131

Special Report 92-2

**U.S. Army Corps
of Engineers**
Cold Regions Research &
Engineering Laboratory

On the Use of an Artificial
Snow Platform for WAM Tests

Donald G. Albert

January 1992

PREFACE

On the Use of an
Artificial Snow Platform for WAM Tests

DONALD G. ALBERT

INTRODUCTION

Because of the lack of a deep snow cover at the February 1991 Wide Area Mine (WAM) ground sensor tests held in Grayling, Michigan, an attempt was made there to simulate the effects of a deeper snow cover by making a pile of snow, compacting it and placing the WAM ground sensor prototype package upon the resulting platform (Fig. 1). Recordings of moving military vehicles were then obtained with these sensors. To investigate the effects of this approach, a test was conducted in Hanover, New Hampshire, a few days later under similar snow conditions, but using a simple acoustic source (a pistol firing blank shots) rather than

moving vehicles. The Hanover tests are described and reported here. The results show that the use of a small snow platform has little effect on the sensor response, and that the Grayling test procedure would be unsuccessful in simulating the effects of a deeper snow cover. The underlying cause of this failure is that the acoustic effect of a snow cover arises over a large areal extent and cannot be simulated by changing the snow properties in a small area near the sensors.

The subsequent section of this report presents the experimental methods used and reports the environmental conditions during the tests. Data analysis and results are presented next, and a discussion of the results follows.

Figure 1. WAM ground sensor prototype on an artificial platform of snow at Grayling, Michigan, 18 February 1991. These sensors were located 75 m from the path of the vehicles (photo courtesy of Steve Decato).

EXPERIMENTAL METHODS

The experiments were conducted at CRREL in Hanover, New Hampshire, on 21 February 1991. The site of the experiments was an open space approximately 100 m long behind CRREL's Frost Effects Research Facility (FERF). This site is relatively flat.

The experiments were conducted by recording acoustic impulses produced by firing blanks from a .45-caliber pistol held horizontally, 1 m above the ground, and pointed toward the sensors. Globe 100C low-frequency microphones were placed on the surface to record the pressures and Mark Products L-15B geophones with a natural frequency of 4.5 Hz were used to record the particle velocity induced at the snow surface by the pistol shots. The sensor outputs were recorded using a Bison Model 9048 digital seismograph; 48 channels were recorded at a sampling rate of 5 kHz, with a bandwidth of 3 Hz to 2.5 kHz.

The data discussed in this report were recorded at two sensor locations (Fig. 2). A microphone and geophone were emplaced in undisturbed snow 75 m from the source location, and served as control sensors (Fig. 3). A snow platform was constructed 85 m away from the source and a geophone and microphone were emplaced on it (Fig. 4). A geophone was also emplaced in undisturbed snow as close to this platform as possible, 84.1 m from the source. Two views of the experimental site are given in Figures 5 and 6. Other sensors were recorded as part of an on-going experimental program, but will not be discussed in this report.

In constructing the snow platform, we tried to duplicate the methods used at Grayling. A wooden frame, 0.91 m square, was fabricated from 2- ×6-in. lumber and pushed down into the snow. Additional snow was then shoveled into the frame and packed down using a cement block (Fig. 7). When the frame was filled to the top, it was removed and more snow was added to taper the edges (Fig. 8). This procedure resulted in a snow layer 16 m thick, with an average density of 545 kg m^{-3} (Table 1). A geophone and microphone were then emplaced at the surface of the platform (Fig. 4).

The shallow, undisturbed snow cover over the test site was continuous except at the bases of posts, where solar loading on the post melted the snow. Two layers were present—an upper layer 0.05 m thick with a density of 270 kg m^{-3} and a lower layer 0.035 m thick with a density of 310 kg m^{-3}. The crystal type for both layers was 6bmf (Colbeck et al. 1990): wet, rounded, melt–freeze polycrystals. There
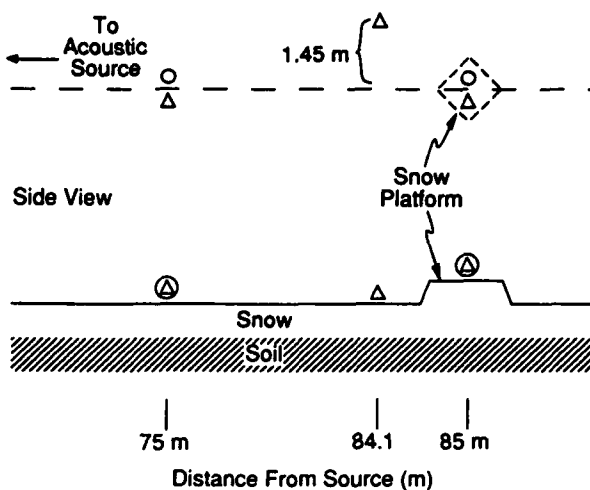
Figure 2. Schematic view (not to scale; circles denote microphones, triangles denote geophones) of the sensors used to record the data. (Top) plan view of the sensor layout; (bottom) cross-sectional view.
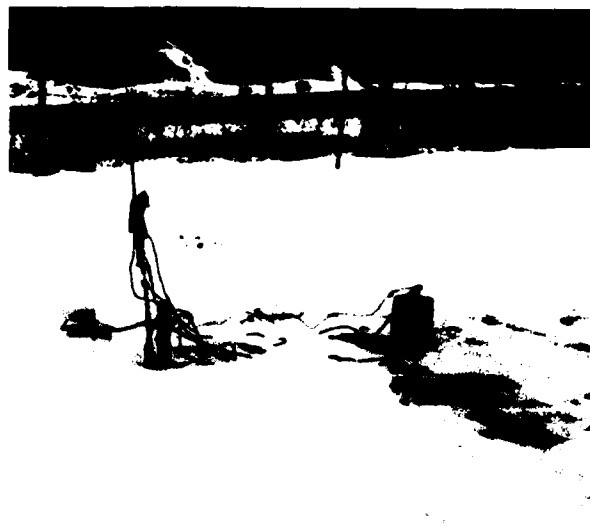
Figure 3. View of the low-frequency microphone and vertical component geophone installed in undisturbed snow 75 m away from the source location. The gray box is a power supply for the microphone.

was also a basal ice layer, 0.015 m thick, present. Table 1 gives the snow cover properties for the undisturbed snow cover and for the snow in the platform. The snow properties are similar to those encountered during the WAM vehicle tests at Gray-

2

Figure 4. A low-frequency microphone and a vertical component geophone in place on the snow platform. These sensors are 85 m from the source location. In the background, a vertical component geophone installed in undisturbed snow is visible; this sensor is 84.1 m from the source point and 1.45 m away (perpendicular) from the direction of pistol fire (i.e., the sensor is 1.0° off the direction of fire).

Figure 5. View of the sensor array looking south (i.e., towards the acoustic source). In the foreground, a vertical component geophone 90 m away from the source is visible. The snow platform, with microphone, power supply and vertical component geophone, is visible along with the geophone installed in undisturbed snow to the right. The large tower is 60 m from the source. A portion of the FERF, with garage door, is visible to the left. This building, and others in the vicinity, cause acoustic reflections to appear on the recorded signals.

Figure 6. View of the test site looking north. The .45-caliber pistol is firing a blank round while being pointed horizontally towards the sensors. The bare ground immediately behind the source location was caused by a plumbing mishap in the FERF. Two small buildings are visible about 100 m away from the source.

Figure 7. Preparing the platform of packed snow for the tests in Hanover, New Hampshire, 21 February 1991. A wooden frame, 0.91 ×0.91 ×0.11 m deep, is being used to keep the snow in place while it is compressed with the cement block.

4

Figure 8. Sides of the snow platform being tapered after removal of the wooden frame by adding and shaping snow along the edges.

Table 1. Snow characterization.

a. Undisturbed snow cover.

Date: 21 Feb 91   Time: 1600   Observer: N.H. Greeley
Cloud cover type: Stratocumulus, 10/10ths coverage.
Air temperature near snow surface (exposed/shaded): 6/6°C.
Snow cover continuous?: Yes, except around base of posts because of solar loading.
Surface clean?: Fairly, little bit of ash from brush burning nearby.
Snow depth range: 4 to 10 cm. Ground frozen?: Yes, depth 8 to 29 cm.

Snowpack profile:

Height above base (cm)		Temp (°C)	Crystal class*	Aggregate size (mm)	Density (kg/m³)
Layer interface	Other				
10		1	6bmf	12 × 8	
	9–6				270
5		1	6bmf	12 × 12	
				12 × 8	
	4–1				310
1.5		0	8cbi		

b. Snow in artificial platform.

Date: 21 Feb 91   Time: 1615   Observer: N.H. Greeley

Snowpack profile:

Height above base (cm)		Temp (°C)	Crystal class*	Aggregate size (mm)	Density (kg/m³)
Layer interface	Other				
16.5		0	6bmf	12 × 6 to	
				20 × 12	
	16–13				550
	12–9				540
	8	0			
	5–2				540
1.5		0	8cbi		

* 6bmf = Rounded, melt–freeze polycrystals; 8cbi = basal ice and hard-packed snow.

Table 2. Meteorological data, 21 February 1991.

Time	Temperatures above and below ground surface (°C)						Wind speed (m/s)			Wind direction (°)**			RH (%)††	BP(mb)††
	−0.03 m	0.01 m	0.08 m	0.28 m	0.98 m	3.0 m*	5 m	3 m	1 m	5 m	3 m	1 m		
0930	−1.3	−1.3	−0.7	0.0	−0.4	−0.6	1.0	†	1.2	215	†	†	47.8	—
1000	−0.1	−0.2	2.8	3.7	3.6	2.8	†	†	0.5	†	†	†	48.6	969
1030	−0.1	−0.1	3.3	4.3	4.2	3.5	†	†	0.8	†	†	†	48.6	953
1100	−0.1	−0.1	3.6	4.7	4.7	3.8	†	†	0.8	†	†	†	48.7	979
1130	−0.1	−0.1	3.6	4.8	4.8	3.8	†	0.6	0.8	†	272	†	48.7	—
1200	0.0	−0.1	3.3	4.5	4.5	4.1	†	0.5	†	†	290	†	48.8	1021
1230	0.0	−0.1	3.2	4.4	4.6	4.6	†	0.5	†	†	46	†	48.8	—
1300	0.0	−0.1	4.0	5.3	5.6	5.2	†	1.1	0.9	†	331	†	49.0	—
1330	0.0	−0.1	4.3	5.4	5.8	5.3	1.6	1.9	1.5	238	245	†	49.0	—
1400	0.0	−0.1	4.5	5.7	6.0	5.6	1.9	2.1	1.8	233	241	†	49.0	—
1430	0.0	−0.1	4.9	6.1	6.3	6.0	1.6	2.0	1.7	220	233	†	49.1	1030
1500	0.0	0.0	4.9	6.1	6.4	6.1	1.4	1.8	1.5	219	222	†	49.2	1023
1530	0.0	0.0	4.3	5.4	5.6	5.3	1.6	1.9	1.7	216	224	†	49.0	1017
1600	0.0	0.0	3.8	4.8	5.0	4.8	1.1	1.4	1.3	212	221	†	48.9	—
1630	0.0	0.0	3.3	4.5	4.7	4.6	†	0.8	0.6	†	206	†	48.9	993

* Depth or height of measurement.
** 0° = north; direction from source (pistol) to the sensor was 315°, 225° is perpendicular to the source–receiver line.
† Below lower limit of the sensors.
†† RH = relative humidity; BP = barometric pressure.

ling. Decato's measurements* of the snow thickness and density for the Grayling platform were 0.105 m and 480 kg m⁻³; for the undisturbed snow the values were 0.165 and 380 kg m⁻³.

The CRREL recordings were made on an overcast, relatively warm day (Table 2). During the tests, the air temperature was 6°C, with 1.5–2 m s⁻¹ winds blowing across the source–receiver line. The shots were all recorded between 1400 and 1530 hours.
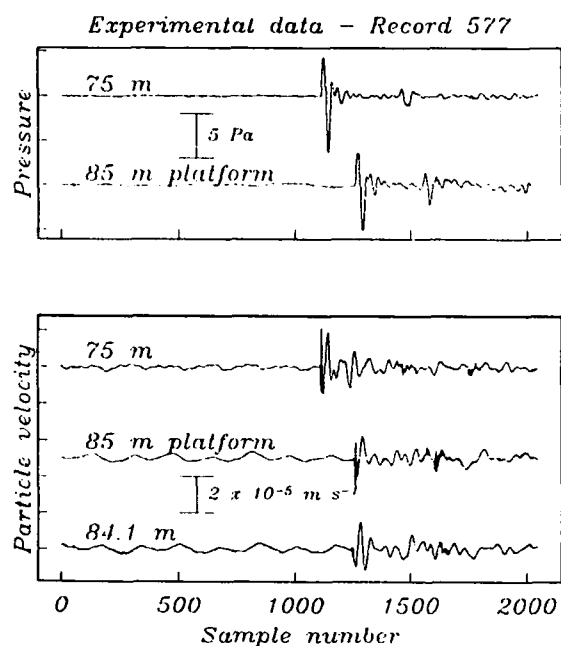
OBSERVATIONS AND DATA ANALYSIS

Examples of the recorded waveforms are shown in Figures 9 and 10. For each of the microphone waveforms, shown in the top of these figures, there is an initial positive pulse representing the pressure increase from the arrival of the air wave (the sound of the pistol shot), followed by a negative pulse and then some smaller oscillations. Another pulse, reflected from one of the nearby buildings, arrives 60–70 ms after the first. The maximum positive pressure is about 5.5 Pa at 75 m, and about

---

* Personal communication with Stephen Decato, CRREL, 1990.

20% less at 85 m. This reduction in amplitude can be entirely accounted for by spherical spreading of the wavefront and the absorption of sound by the snow cover (Albert and Orcutt 1989). A major result of these tests can be pointed out here: placing a microphone on a small platform of snow has no effect on the recorded waveform.
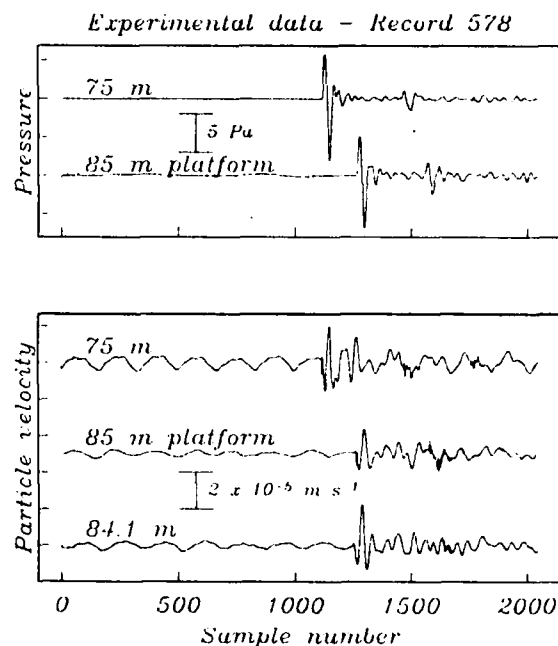
The vertical component geophone signals are shown in the lower portion of Figures 9 and 10. The initial motion for these waveforms is downward and is a result of the pressure induced on the snow surface by the passage of the air wave. This initial downward impulse is followed by a large upward pulse (rebound of the surface), and then by a train of decreasing oscillations. The later reflected pulses are also visible on the geophone signals. The noise level is much higher for the geophones than for the microphones, as can be seen by examining the early part of the traces in Figure 9 that occur before the arrival of the air wave. This noise is caused by machinery operating in the FERF and by vehicles moving about nearby. To improve the signal-to-noise ratio of the geophones, five pistol shots were summed for some records, Figure 10 being one example that illustrates the improvement in the data quality.

The geophone signals show a very high-frequency oscillation when the air wave arrives. These oscillations vary from one record to another, with Fig-

Experimental data — Record 577

Experimental data — Record 578

a. Recorded at 1448 hours on 21 February 1991.

b. Recorded at 1449 hours on 21 February 1991.

Figure 9. Microphone (top) and vertical component geophone (bottom) signals recorded for a single .45-caliber blank pistol shot. The sample interval was 0.2 ms.
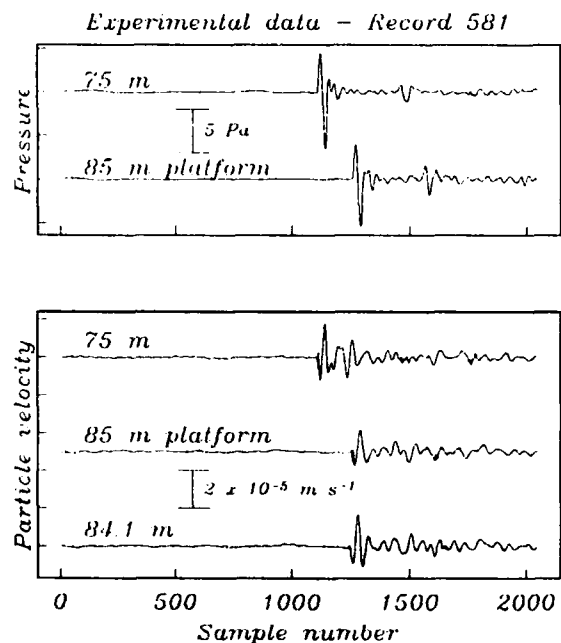

Experimental data — Record 581

Figure 10. Microphone (top) and vertical component geophone (bottom) signals recorded by summing five .45-caliber blank pistol shots, recorded at 1455 hours on 21 February 1991.

ure 9a showing the largest oscillations of the 25 data records obtained, and with the oscillations of Figure 9b (recorded within 1 minute of Fig. 9a) being more typical. This part of the signal is the "blast" wavefront, and its appearance is highly dependent on the instantaneous atmospheric conditions and the presence of turbulence.

To examine the frequency content of the recorded waveforms, the power spectra of the signals were calculated. Because of the short data series, the multiple window technique (Thomson 1982) was employed for these calculations. Figure 11 shows that the initial pulse is composed of frequencies from about 500 to 2500 Hz. These high-frequency signals do not appear on the microphones, since their sensitivity drops at these high frequencies (down by about a factor of two at 500 Hz).

Comparing the geophone signals for the different geophones in Figures 9 and 10 reveals only slight differences. The waveform for the geophone located on the snow platform is of slightly lower amplitude than the waveform for the geophone located on undisturbed snow nearby. The ratio of the maximum for the platform geophone at 85 m to the geophone at 84.1 m is 0.89 ± 0.12 (95% confidence interval) for 25 shots. This difference is not
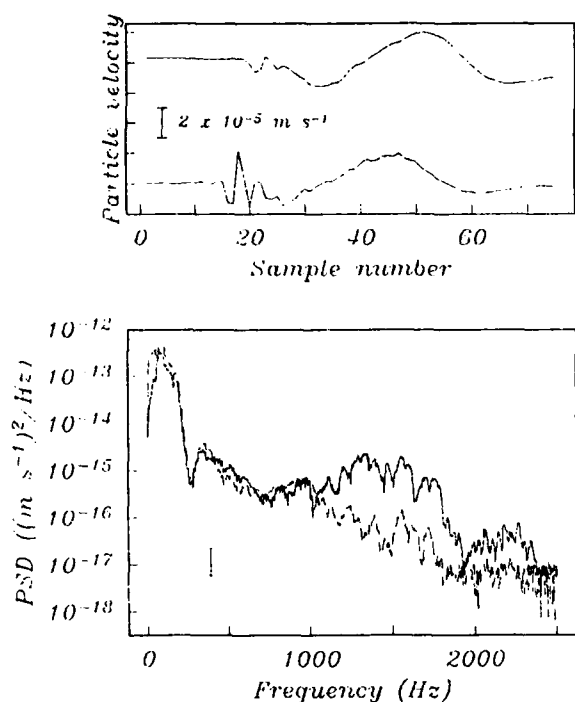
7

Figure 11. Response of a vertical component geophone in undisturbed snow to a single .45-caliber blank pistol shot 75 m away. The top panel shows the two time series recorded by this geophone for the shots shown in Figure 9a (bottom trace) and 9b (top trace). The sample interval was 0.2 ms. The bottom panel shows the power spectral density computed for the time series, with a vertical bar indicating the 95% confidence interval. The solid line is for the bottom trace of the top panel; the dashed line is for the top trace. The difference between the two spectra is from the differences in the initial, high-frequency arrival visible in the time series data.
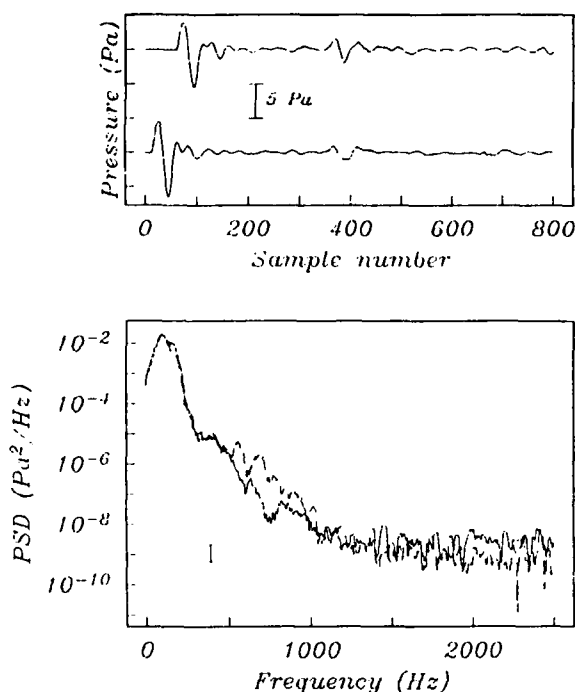
Figure 12. Power spectra for the microphone signals shown in Figure 10. The top panel shows the time series recorded by the microphone on the snow platform at 85 m (top) and on undisturbed snow at 75 m (bottom). The bottom panel shows the power spectral densities computed for these time series, with a vertical bar indicating the 95% confidence interval. The solid line is for the microphone at 75 m, the dashed line is for the microphone at 85 m. These spectra are nearly identical.

significant because the sensitivity of geophones varies within that range. This observation is another major result of these tests: the snow platform has little effect on the geophone signals.

The acoustic-to-seismic-coupling ratios were determined by dividing the maximum pressure measured by a surface microphone into the initial downgoing particle velocity measured by a surface geophone. The ratios were $(2.9 \pm 0.2) \times 10^{-6}$ m s^{-1} Pa^{-1} for the sensors in undisturbed snow at 75 m and $(2.3 \pm 0.1) \times 10^{-6}$ m s^{-1} Pa^{-1} for the sensors on the snow platform at 85 m. These ratios agree within the accuracy of the measurements. Previous measurements (Albert 1990) have also shown that there is little variation in geophone coupling to snow of various physical characteristics.

Figure 12 shows the power spectra calculated for the microphone waveforms recorded by stacking

five blank pistol shots. The spectra for the two microphones, located 75 and 85 m away from the source, are essentially identical, and most of the energy is contained in the band below 200 Hz. The higher frequencies are absorbed by the snow cover (Albert and Orcutt 1990).

Figure 13 shows the power spectra for the geophones located in undisturbed snow and on the snow platform. These spectra have the same spectral shape as the microphone spectra in the previous figure, as expected, since acoustic-to-seismic coupled energy is the dominant energy recorded by these sensors. Above 1 kHz, where the signal is three orders of magnitude less than the peak, the geophone on the snow platform shows a higher spectral level than the one in undisturbed snow. There are two likely causes of this difference. First, large variations in the high-frequency response of
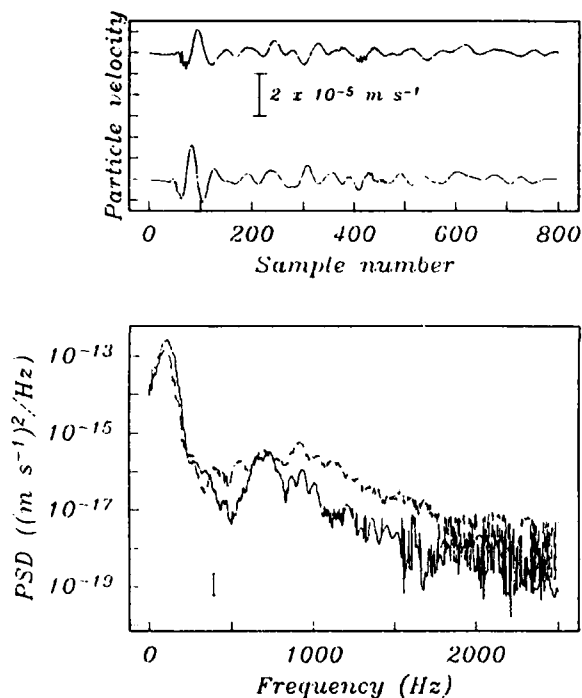
8

Figure 13. Power spectra for two of the geophone signals shown in Figure 10. The top panel shows the time series recorded by the geophone on the snow platform at 85 m (top) and on undisturbed snow at 84.1 m (bottom). The bottom panel shows the power spectral densities computed for these time series, with a vertical bar indicating the 95% confidence interval. The solid line is for the geophone on undisturbed snow, the dashed line is for the geophone on the platform.
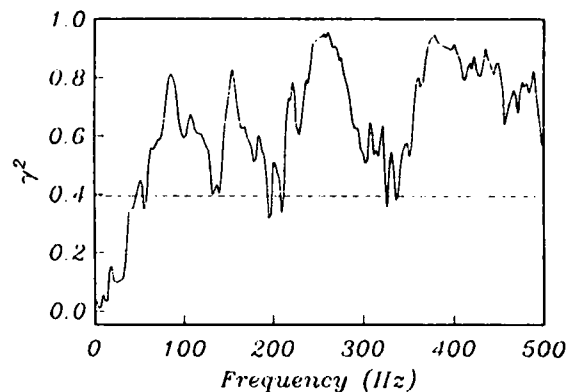
Figure 14. Magnitude squared coherence calculated for the microphone and geophone located on the snow platform at 85 m, for the signals shown in Figure 10. A value of γ > 0.4 indicates that the coherence is significantly different from zero at the 95% confidence level.
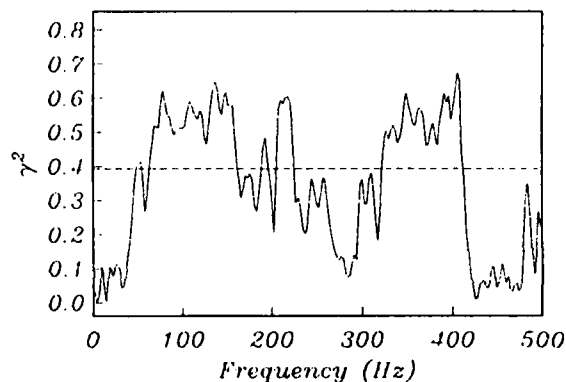

Figure 15. Magnitude squared coherence calculated for the geophone located in undisturbed snow at 84.1 m, and the geophone located on the snow platform at 85 m, for the signals shown in Figure 10. A value of γ > 0.4 indicates that the coherence is significantly different from zero at the 95% confidence level.

the geophones are possible, since this frequency band is well outside the manufacturer's design range. Second, coupling of the geophones to the snow can also have an influence, and an 0.08-m-long spike was used on the platform geophone, while a plastic base plate without a spike was used on the other geophone. The differences in high-frequency response for these two geophones are measurable, but would have little influence in vehicle detection or identification since the signal levels are very low at these frequencies.

To examine the linear relation between two time series, one can calculate the magnitude squared coherence

$$\gamma^2 = X_{12}^2 / [X_{11} X_{22}]$$

where X_{ii} is the power spectrum of the ith time series and X_{ij} is the cross-spectrum between the ith and jth time series. Figure 14 shows the squared coherence between the microphone and the geo-

phone located on the snow platform. This plot shows that there is a strong linear relation between the two sensors for the frequencies from 50 to 500 Hz, confirming the importance of acoustic-to-seismic coupling on the geophone signal. There is very little acoustic energy produced by the pistol shot below 50 Hz, and the geophone signal is mostly from seismic background noise, so the two sensors are uncorrelated at low frequencies.

Figure 15 shows the coherence for the geophones on undisturbed snow and on the snow platform. In this case, there is strong coherence in the 0- to 150- and the 300- to 400-Hz frequency bands.

9

DISCUSSION

Snow on the ground can have major effects on the performance of acoustic and seismic ground sensors. The primary effect is from absorption of airborne sound by the snow cover, which results in a reduction in the overall sound pressure level. This absorption occurs mainly at frequencies above 100 Hz, so the snow cover acts as a lowpass filter, and causes the initially broad spectrum of the pistol shot to be transformed to the shape of the acoustic spectra seen in Figure 12, where the low frequencies are three orders of magnitude larger than the high frequencies. Field measurements have shown the sound pressure level reduction to be greater than an order of magnitude for propagation over 100 m of snow (Albert and Orcutt 1990). This reduction is caused by the continuous interaction of acoustic waves with the snow cover over the entire travel path of the waves. The effect is not simulated by a small area of thicker snow near the sensors. Conversely, clearing snow away from a small area around a ground sensor package would not reduce this attenuation.

Although one might expect the snow cover to affect acoustic-to-seismic-coupling ratios, field measurements have shown that the coupling ratio for snow is similar to that of soils without snow (Albert and Orcutt 1989, Albert 1990). The induced signal measured by a geophone is lower in amplitude and lowpass filtered. These changes are caused by the attenuation of the airborne sound wave as it propagates over the snow cover, not by differences in the elastic properties of snow compared to soil. Of course, some variation in this ratio is expected for snow with different elastic moduli (see Albert 1990, for examples), but even the compaction of the snow in constructing the platform for the experiments reported here was not sufficient to significantly affect the ratio compared to the undisturbed, relatively high density snow already present at the site.

The phenomenon of acoustic-to-seismic coupling, or transfer of energy from airborne waves into ground motion, occurs continuously as acoustic waves propagate over the ground surface. The actual surface area involved in the coupling, and influencing the response of a geophone, has not been directly measured, but some information can be obtained from previous studies. Sabatier et al. (1986) performed experiments by placing sensors in holes of various sizes filled with pumice, a very low density, porous material. They used continuous wave, single-frequency sources, and the enhancements they measured appear to be ascribable to resonances within the hole, which had nearly rigid walls. These effects were observed for holes with surface areas of 1 m² or greater. Van Hoof (1986) also conducted similar experiments, and found similar coupling areas.

For the experiments reported here, the boundary conditions are different from those of Sabatier et al. (1986) since the snow platform is surrounded by air rather than by rigid walls. For assumed boundary conditions of a free surface at the top and side walls and a rigid bottom, the resonant frequencies' normal modes within a rectangular box are

$$f_{ijk} = (c/2)\left[(i/x_1)^2 + (j/x_2)^2 + ((2k-1)/x_3)^2\right]^{1/2}$$

where i, j and k are the mode numbers and x_i the dimensions of the box. Since the box in the experiment was aligned obliquely with the source, the lowest modes expected are $f_{110} = 385$, $f_{001} = 516$ and $f_{111} = 630$ Hz, where a wave speed of 330 m s⁻¹ in the snow has been assumed. (An assumed wave speed of 100 m s⁻¹ would lower these frequencies to 110, 156 and 191 Hz respectively.) There are no spectral peaks from resonances at these or at any other frequencies visible in the geophone spectra of Figure 13, so vibrations within the platform are not significant in these experiments, unlike those of Sabatier et al. (1986).

Berry and Attenborough (1988) conducted laboratory measurements by sliding rigid plates over a soil surface and measuring the spectrum of waves reflected (at a 45° angle) from that surface. This method eliminates the resonance effects. By examining their data, I estimate that 1 to 2 wavelengths of surface in the direction of propagation are needed to significantly affect the acoustic-to-seismic coupling. At 100 Hz, this corresponds to 3–7 m along the surface, compared to the 1.3-m length of the snow platform used in the winter experiments. These estimates indicate that a much larger platform would need to be constructed to affect the acoustic-to-seismic coupling.

CONCLUSIONS

Experimental measurements show that using a small platform constructed of snow is not an effective method of simulating a thick snow cover. The measurements showed no effect on the waveforms recorded by microphones and geophones placed on the platform, and the acoustic-to-seismic coupling ratio was also unchanged. In addition, no

10

resonant reverberations within the snow platform were observed.

LITERATURE CITED

Albert, D.G. (1990) Preliminary analysis of measured sound propagation over various seasonal snow covers. In *Proceedings of the Fourth International Symposium on Long Range Sound Propagation, 16–17 May 1990, Hampton, Virginia.* Washington, D.C.: National Aeronautics and Space Administration, NASA CP-3101, p. 51–57.

Albert, D.G. and J.A. Orcutt (1990) Acoustic pulse propagation above grassland and snow: Comparison of theoretical and experimental waveforms. *Journal of the Acoustical Society of America,* **87**: 93–100.

Albert, D.G. and J.A. Orcutt (1989) Observations of low frequency acoustic-to-seismic coupling in the summer and winter. *Journal of the Acoustical Society of America,* **86**: 352–359.

Berry, D.L. and K. Attenborough (1988) Area of ground influencing sound propagation from a point source. In *Proceedings of the Third International Symposium on Long Range Sound Propagation and Coupling into the Ground, 28–30 March 1988, Jackson, Mississippi.* University of Mississippi Report, p. 143–151.

Colbeck, S.C., E. Akitaya, R. Armstrong, H. Gubler, J. Lafeuille, K. Lied, D. McClung, and E. Morris (1990) *The International Classification for Seasonal Snow on the Ground.* International Commission on Snow and Ice of the International Association of Scientific Hydrology. Cambridge, U.K.: International Glaciological Society.

Sabatier, J.M., H.E. Bass and G.R. Elliott (1986) On the location of frequencies of maximum acoustic-to-seismic coupling. *Journal of the Acoustical Society of America,* **80**: 1200–1202.

Thomson, D.J. (1982) Spectral estimation and harmonic analysis. *Proceedings of the IEEE,* **70**: 1055–1096.

van Hoof, H.A.J.M. (1983) Acoustic and seismic measurements in seismic boxes. The Hague, The Netherlands: National Defense Research Organization, Physics and Electronics Laboratory, Report No. FEL 1986-47.

1. AGENCY USE ONLY (Leave blank)	2. REPORT DATE January 1992	3. REPORT TYPE AND DATES COVERED

4. TITLE AND SUBTITLE

On the Use of an Artificial Snow Platform for WAM Tests

5. FUNDING NUMBERS

ARDEC Contract #W81EF-1-M019

6. AUTHORS

Donald G. Albert

7. PERFORMING ORGANIZATION NAME(S) AND ADDRESS(ES)

U.S. Army Cold Regions Research and Engineering Laboratory
72 Lyme Road
Hanover, New Hampshire 03755-1290

8. PERFORMING ORGANIZATION REPORT NUMBER

Special Report 92-2

9. SPONSORING/MONITORING AGENCY NAME(S) AND ADDRESS(ES)

U.S. Army Armament Research, Development and Engineering Center
Picatinny Arsenal, New Jersey

10. SPONSORING/MONITORING AGENCY REPORT NUMBER

11. SUPPLEMENTARY NOTES

13. ABSTRACT *(Maximum 200 words)*

An experiment was conducted to test the effectiveness of using a small platform constructed of packed snow to simulate the effects of a snow cover on ground sensors used in vehicle detection and identification. A simple impulsive acoustic source (.45-caliber pistol firing blanks) was used to simplify the interpretation of the experimental measurements. Geophones and microphones on the snow platform and on undisturbed snow nearby were used to record the signals. These measurements show no significant difference between signals recorded on the snow platform and on the surrounding undisturbed snow. Consideration of previous measurements and acoustic theory shows that the platform would have to be much larger in areal extent to affect the recorded signatures; it is the interaction of the acoustic waves with the ground surface over their entire propagation path that controls the properties of the signal at the ground sensor.

14. SUBJECT TERMS		15. NUMBER OF PAGES 17
Acoustic-to-seismic coupling Cold regions Snow acoustics Sound attenuation	Wave propagation Wide Area Mine (WAM) Winter warfare	16. PRICE CODE

17. SECURITY CLASSIFICATION OF REPORT	18. SECURITY CLASSIFICATION OF THIS PAGE	19. SECURITY CLASSIFICATION OF ABSTRACT	20. LIMITATION OF ABSTRACT
UNCLASSIFIED	UNCLASSIFIED	UNCLASSIFIED	UL